Environmental Science Nano

ROYAL SOCIETY OF CHEMISTRY

PAPER

View Article Online
View Journal | View Issue

Check for updates

Cite this: *Environ. Sci.: Nano*, 2025, 12, 2357

Blue micro-/nanoplastics abundance in the environment: a double threat as a Trojan horse for a plastic-Cu-phthalocyanine pigment and an opportunity for nanoplastic detection *via* micro-Raman spectroscopy†

Ioana Cârdan, [abc] Ion Nesterovschi,[ab] Lucian Barbu-Tudoran[c] and Simona Cîntă Pînzaru*[ab]

Received 4th September 2024,
Accepted 12th February 2025

DOI: 10.1039/d4en00820k

rsc.li/es-nano

Blue plastics, whether macro- or micro-sized, are intriguingly frequently reported in significant numbers of studies dealing with the contamination of environmental waters or living organisms with microplastics. In our recent investigations on microplastics in environmental waters, we noted abundant blue microfibers and fragments, whose identification was achieved *via* Raman spectroscopy. Still widely used in the plastics industry, despite awareness raised at a global level, copper phthalocyanine (CuPc), a blue pigment carried by abundantly used blue plastics, like a "Trojan horse", is a secondary threat (after plastics) in the trophic chain, being highly resistant to a broad range of conditions. Here, the newly discovered resonance Raman (RR) signal of the blue pigment CuPc embedded in environmentally aged plastics allowed us to lower the minimum size of detectable nanoplastics *via* micro-Raman spectroscopy down to 500 nm. In addition, we demonstrated nanoplastics detection solely *via* the CuPc RR signal, a result subsequently validated using SEM–EDX. Based on a visible-NIR Raman spectroscopy investigation of isolated synthetic CuPc compounds, we discussed the observed changes in pigment spectra in blue plastic waste aged for an estimated 20 years, consisting of highly brittle ropes knotted in fishing nets and harvested *via* scuba diving from the seabed. Thus, the fate of CuPc in environmentally aged blue plastics could provide robust analytical opportunities when studying the impact of aged, blue-coloured plastics at various levels, due to its persistent, selective and specific RR signal. The results are crucial for expanding the capability of Raman tools for further tracking the micro-to-nanoplastic degradation of waste along the trophic chain, improving our understanding of its impact on living organisms.

Environmental significance

Although nanoplastic detection in environmental ecosystems has apparently been reported, in fact, a method to detect evidence of environmentally aged nanoplastics is absent. In this study, we provide the first demonstration of the detection of blue nanoplastics originating from years-old plastics recovered from the seabed. The successful detection of environmentally aged blue nanoplastics is based on the newly discovered resonance Raman signal of the copper phthalocyanine pigment embedded in plastics. Therefore, by combining the resonance Raman effect of blue pigmented nanoplastics and confocal Raman spectroscopy, an effective analytical tool is provided for tracing and monitoring nanoplastics in the environment. Furthermore, this tool could also find application in studies that are highly relevant for the environment, such as investigating the impact of aged and pigmented nanoplastics on the environment and biota.

Introduction

According to the *International Organization for Standardization* (ISO/TR 21960:2020)[1] microplastics (MPs) and nanoplastics (NPs) are considered plastic particles in the size range of 1 μm–5 mm and 1 nm–1 μm, respectively. They are considered to be emerging environmental pollutants, accumulating across various trophic levels and leading to multiple ecological repercussions.[2] To date, microplastics have been

[a] *Faculty of Physics, Babeș-Bolyai University, Kogălniceanu 1, 400084 Cluj-Napoca, Romania. E-mail: simona.pinzaru@ubbcluj.ro*
[b] *RDI Laboratory of Applied Raman Spectroscopy, RDI Institute of Applied Natural Sciences (IRDI-ANS), Babeș-Bolyai University, Fântânele 42, Cluj-Napoca 400293, Romania*
[c] *National Institute for Research and Development of Isotopic and Molecular Technologies, Donath 67-103, 400293 Cluj-Napoca, Romania*
† Electronic supplementary information (ESI) available. See DOI: https://doi.org/10.1039/d4en00820k

widely detected in various environmental compartments. They have been found in human blood,[3] human placentas[4] and in marine life, ranging from tiny plankton to large whales.[5–8] Moreover, their existence has been reported in the atmosphere[9] of terrestrial environments,[10] as well as in bodies of water, including mountain spring water,[11] freshwater[12,13] and even in drinking water.[14] The presence of nanoplastics in drinking water has been also reported in recent studies.[15,16]

Interestingly, a significant number of studies[17–26] have reported a high abundance of blue microplastics, these being particularly prevalent in aquatic environments.[27] All these studies concerning plastic contamination in various environments have reported predominantly blue microfibers or fragments. Moreover, our recent study[11] regarding the contamination of spring water with microplastics also reported a high abundance of blue microparticles, whose origin is thought to come from agricultural plastic fragments during soil drainage. We determined that a particular Raman signal originating from the analyzed blue macro- and microplastics corresponds to a combination of polymers and blue-pigment Raman bands, which are laser-excitation dependent. Thus, many micro-fragments or fibers of suspicion found in freshwater bodies, such as rivers or spring water,[11] were identified with Raman based on the specific signature of the copper phthalocyanine (CuPc) pigment. As part of our input into the national campaign "*Romania, I love you! Romania on PET*",[28] a first-of-its-kind journalistic endeavor based on eloquent laboratory analysis, we revealed abundant microplastic fragments from real-world samples, randomly collected from rivers; of these, the blue microplastic dominance was remarkable.

Since 1928 when phthalocyanines were accidentally discovered, they have become the second-most important class of colorants. They were found to be organic compounds,[29] and their great commercial impact is mainly based on three properties: bright-blue to green colors, chemical stability and excellent fastness to light.[30] The copper derivatives of phthalocyanines, named copper phthalocyanines (CuPcs), have been demonstrated to be the most stable blue, green and cyan pigments.[31] Based on their great properties as intense colors, great technical performance and low cost,[32,33] the use of CuPc pigments was estimated to be divided as follows: 42% in printing inks, 30% in paints, 20% in plastics, and the rest in textiles, photographs and other products.[34] Copper phthalocyanine pigments exhibit polymorphism and two important polymorphs are the alpha (α) and beta (β) forms.[35] The β form is a greenish-blue one with applications especially in printing inks as a cyan pigment, and the α form is reddish blue, being important for applications in paints and plastics.[36] The unstable/non-stabilized alpha crystal phase of CuPc is known as Pigment Blue 15 (PB15). Upon its stabilization, various other α and β forms of CuPc are obtained: Pigment Blue 15 : 1 (PB15 : 1), Pigment Blue 15 : 2 (PB15 : 2), Pigment Blue 15 : 3 (PB15 : 3), Pigment Blue 15 : 4 and Pigment Blue 15 : 5.[37] The Pigment Blue 15 : *x* forms of copper phthalocyanines are by far the most widely used blue pigments,[34] offering properties such as light and color fastness, homogeneity, chemical and physical stability, excellent weathering and high color strength.[38] Taking into account all these characteristics, PB15 pigments appear to be an ideal choice for the marketplace, particularly for use in plastic-coloring applications.[39]

However, the presence of high levels of blue micro- and nanoplastics could represent a double danger to the environment, first because of the small size and high surface area of the plastic itself and then because of the pigment content. While CuPc itself is classified as low in toxicity for humans and aquatic life due to its low solubility and stability, recent research[40] shows increased environmental risks when CuPc leaches from aged plastics. Specifically, CuPc exacerbates oxidative stress in cyanobacteria (*Microcystis aeruginosa*), leading to elevated superoxide dismutase (SOD) activity and malondialdehyde (MDA) levels, which indicate cellular and membrane damage. Martí *et al.*[41] proposed two explanations as to why bluish plastic items are present in such high proportions in the marine environment and about the danger posed. One explanation proposed is that bluish plastic particles are removed on a lesser scale from the surface by plastic-ingesting predators[42] compared with other colors, resulting in a higher accumulation of bluish plastic particles. Another explanation suggests that abundantly used bluish fishing lines may fragment, leading to the accumulation in the environment of small micro- and nanosized blue fragments and filaments. Therefore, their detection and monitoring in the environment is essential for understanding their effect in trophic chains. In this regard, Raman spectroscopy coupled with confocal microscopy is a suitable method to approach both challenges. Raman spectroscopy is well-documented as a method of choice for plastics and pigment identification[43,44] and sorting[45–47] and microplastics screening in environmental compartments.[48]

Even if micro-Raman spectroscopy prevails in terms of its advantages for microplastics analyses, when it comes to analyzing nanoplastics, the limitations of Raman spectroscopy make their trace detection more challenging, with nanoplastics being an "invisible" threat. Moreover, the detection of environmental nanoplastics presents an even greater challenge,[49] as they could be mixed with other inorganic and organic matter, such as environmental biofilms and micro-organism metabolites,[50] decomposition products, residual contaminants from the primary human utilization of respective plastic products and a combination of these. Among the techniques reported for detecting nanoplastics,[49] spectroscopic techniques are particularly preferred.[51]

Regarding spectroscopic techniques and their interlaboratory validation in response to EU and US directives to control microplastics in drinking water,[52] Raman spectroscopy is generally ruled out, as "Raman spectroscopy

has a reported resolution limit of ~1 μm that hinders its use for detecting submicron and nanoplastic particles".[53,54] This perception should be revised, and we provide here evidence in this regard.

Developed Raman-based techniques,[55,56] such as surface-enhanced Raman scattering (SERS) spectroscopy[57,58] resonance Raman (RR) spectroscopy, Raman imaging, and their combination can overcome the weak sensitivity of normal Raman spectroscopy. As of May 24, 2024, searching the keywords *SERS + NANOPLASTIC* on Web of Science (WoS) revealed 10 articles, which usually used standard commercially available nanoplastics, predominantly polystyrene spheres. Further studies supporting the SERS-based development of nanoplastics tracking in real-world samples (not spiked and subsequently detected) are in their infancy. In this regard, our new SERS platforms under development could be promising and will be addressed elsewhere (Marica *et al.*, in preparation).

Here, by making use of RR spectroscopy,[55] we enabled the detection of blue nanoplastics naturally fragmented down to 500 nm, which bear a strong Raman signal specific to the CuPc blue pigment, industrially known as PB15, embedded in a polymer matrix.

We i) first assessed here the appearance and variability of the PB15 Raman signal and its dependencies in blue and naturally degraded macro-, micro- and nanoplastics, and ii) further exploited this to lower the size limit for plastic detection by micro-Raman spectroscopy. The nanoplastics analyzed here are blue rope samples aged for 20 years, knotted in fishing nets, harvested *via* scuba-diving from the seabed in a traditional shellfish farming area. Based on the RR signal of PB15 we were able to detect environmental blue plastic fragments in the nanometer range (below 1 μm). Moreover, we show that naturally occurring blue nanoplastics show only the CuPc pigment signal, therefore, their detection could be performed based only on the pigment signal. Thus, here we present a robust analytical alternative for the unambiguous detection of environmentally abundant blue nanoplastics *via* the RR signal of a specific copper phthalocyanine pigment. The present findings will contribute to improved methods for tracking micro-to-nanoplastic degradation along the trophic chain, which is currently of increasing interest for understanding the impact of micro- and nanoplastics on various organisms.

Materials and methods

CuPc pigments and blue plastic samples collection

Copper phthalocyanine has been obtained courtesy of Dr. Luiza Gaina from the Department of Chemistry, Babeș-Bolyai University, Cluj-Napoca, which recently investigated a phthalocyanine derivative for the development of therapeutic agents.[59]

The collection of blue plastic samples includes 107 plastic waste samples from macro- to micrometer range. The macroplastics consist of 26 blue and green plastic waste items (Fig. 1a) covering 4 types of plastics: low-density polyethylene (LDPE), high-density polyethylene (HDPE), polypropylene (PP), and polystyrene (PS). These are plastic

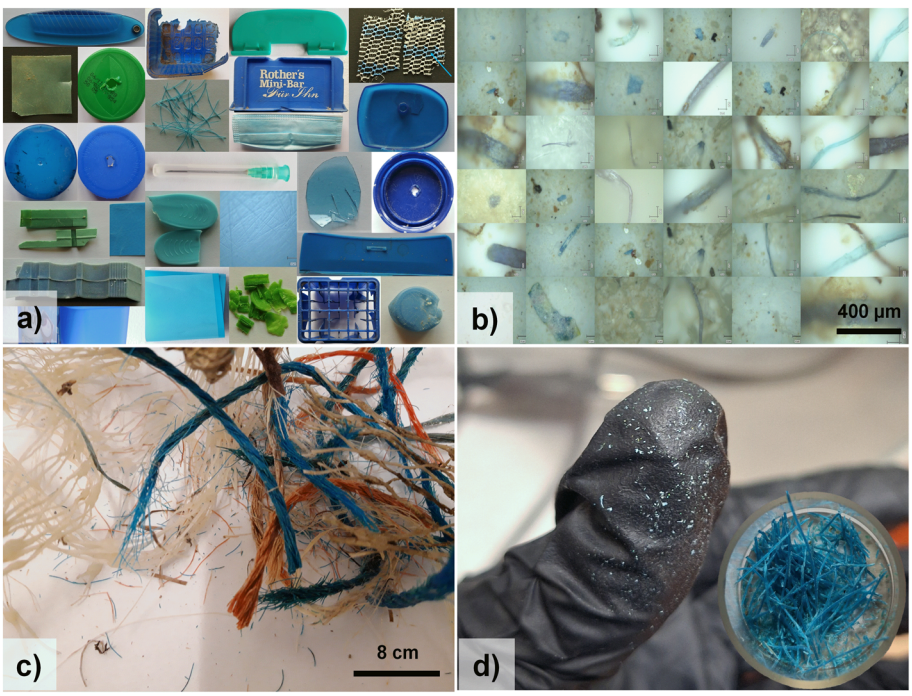

Fig. 1 A collection of images illustrating typical blue and green a) macroplastics and b) microplastics; c) coloured ropes collected from the sea; and d) separated blue rope, highlighting its natural fragmentation into blue microplastics and nanoplastics.

items naturally degraded by environmental and indoor conditions and were collected from various environmental matrices/compartments. The detailed characteristics and properties of each sample are precisely described in our plastic Raman database.[60] Additionally, to simplify the process of searching within the database for each sample, the sample names used in the Results section match those indexed in our database.

The 81 blue microplastics (a few examples are shown in Fig. 1b) analyzed here originated from the filtration of high quantities of environmental water from three different areas in Romania, resulting in different batches of microplastics. The first was obtained from the filtration of spring water from two karst springs (*Josani and Albioara*) located in the *Apuseni* Mountains in Romania. The detailed sampling procedure is described in our recent paper.[11] The second batch originates from water filtration of both the *Someș* river in an urban area of Cluj county, Romania, and a highly polluted area of Romania, the *Homorord* river, which was the subject of a journalistic investigation that was finalized in a scientific documentary entitled "*Romania, I love you, Romania on PET*".[28] The microplastics retained on Millipore filters were further analyzed.

The blue nanoplastics analyzed are particles resulting from the natural degradation of blue filaments of polypropylene on the seabed (Fig. 1c). Several images of blue PP are included in our plastic Raman database, under the sample code PP-BL-003.[61] The stock of blue filaments of polypropylene were collected (recovered) from the seabed, *via* scuba diving, in June 2019 from the Bay of Bistrina on the South Adriatic coast, where intensive shellfish farming is traditional. The plastics consisted of several blue ropes, knotted with other white-grey nets and red-coloured ropes (Fig. 1c). They were deposited in a large sampling vial without any cleaning and transported to the laboratory and stored in cool and dark conditions. The raw plastic waste collected from the sea was preserved under lab conditions and, to date, it has spent 5 years in the lab, while according to the model used in local aquaculture farming, aquaculture experts estimated about 15 years of ageing in seawater at the time of sampling; thus, the plastic is further assumed to have aged for 20 years in the present study.

When random blue-coloured filaments were taken from the sampling vial for analyses (Fig. 1d)), their high susceptibility to fragmentation was observed. When exposed to marine aquatic conditions, where mechanical, biochemical, photo- and thermo-oxidative degradation processes apply, plastics become more brittle and easily fragmented over time.[62,63] Thus, the macro-fibers (ropes) recovered from the seabed after years of degradation under marine conditions became spontaneously brittle upon handling to leave micro-/nanosized fragments in the collection vial in powder form. These spontaneously formed powders arising in the vials of the harvested seabed plastics were the subject of the present analysis.

Blue plastics analysis

Raman analysis was performed using a Renishaw InVia Reflex confocal Raman spectrometer with laser light excitation from the UV to NIR region. For our measurements, we used 785 nm, 632.8 nm and 532 nm laser light excitation with corresponding nominal powers of 300 mW, 17 mW and 200 mW, respectively. The excitation wavelength and the respective power used are specified in each figure caption. The spectrometer is equipped with a RenCam CCD detector (1024 × 256 pixels, 200–1060 nm) for visible light and an InGaAs (800–1660 nm) detector for NIR. A 1800 lines per mm grating for visible excitation wavelengths (532 nm and 632.8 nm) and 1200 lines per mm grating for 785 nm light were automatically employed using Wire 3.4 software. The spectral resolution was 0.5 cm^{-1} for 532 and 632.8 nm and 1 cm^{-1} for 785 nm. For the analysis of macro- and microplastics, the laser was focused with a 20x magnification objective (NA 0.35). In the case of nanoplastics, a 100× magnification objective (NA 0.9) was used. The nanoplastics were identified upon conducting Raman measurements on fragments that were still detectable as dots under 100× objective magnification *via* confocal Raman microscopy.

The nano-/micro-size distribution of blue plastic particles has been demonstrated *via* micro-Raman and scanning-electron microscopy (SEM)/transmission-electron microscopy (TEM) coupled with energy dispersive X-ray spectroscopy (EDX) analyses. The SEM/TEM-EDX measurements indicated a wide nanometer-size distribution.

The conversion of the collected Raman spectra into spectroscopic barcodes has done according to the method described by Velioglu *et al.*[64]

Results and discussion

Resonance Raman spectroscopy analysis of the copper phthalocyanine pigment

Copper phthalocyanine exhibits two main absorption bands, the B-band in the near-UV range and the Q-band in the visible spectrum. The Q-band consists of a wide band at 611 nm, a shoulder at 645 nm, and another band at 718 nm.[65,66] These bands are part of the $\pi \rightarrow \pi^*$ transition within the π-system comprising C and N atoms.[67–69] Considering the well-known UV-vis absorption of CuPc in the visible region, we analyzed the pigment using three laser wavelengths, 532 nm, 632.8 nm, and 785 nm. The RR effect occurs when the excitation laser wavelength falls within the electronic absorption band of the molecule. Given that the RR effect involves using a laser excitation wavelength very close to the molecule's electronic absorption maximum, we anticipate an additional RR enhancement of the functional groups responsible for the chromophore of CuPc when using the 632.8 nm laser, thus allowing selective detection of the specific RR band.

The experimentally measured Raman spectra of copper phthalocyanine at the three wavelengths are illustrated in Fig. 2a and b within the range of 150–3200 cm^{-1} and 650–

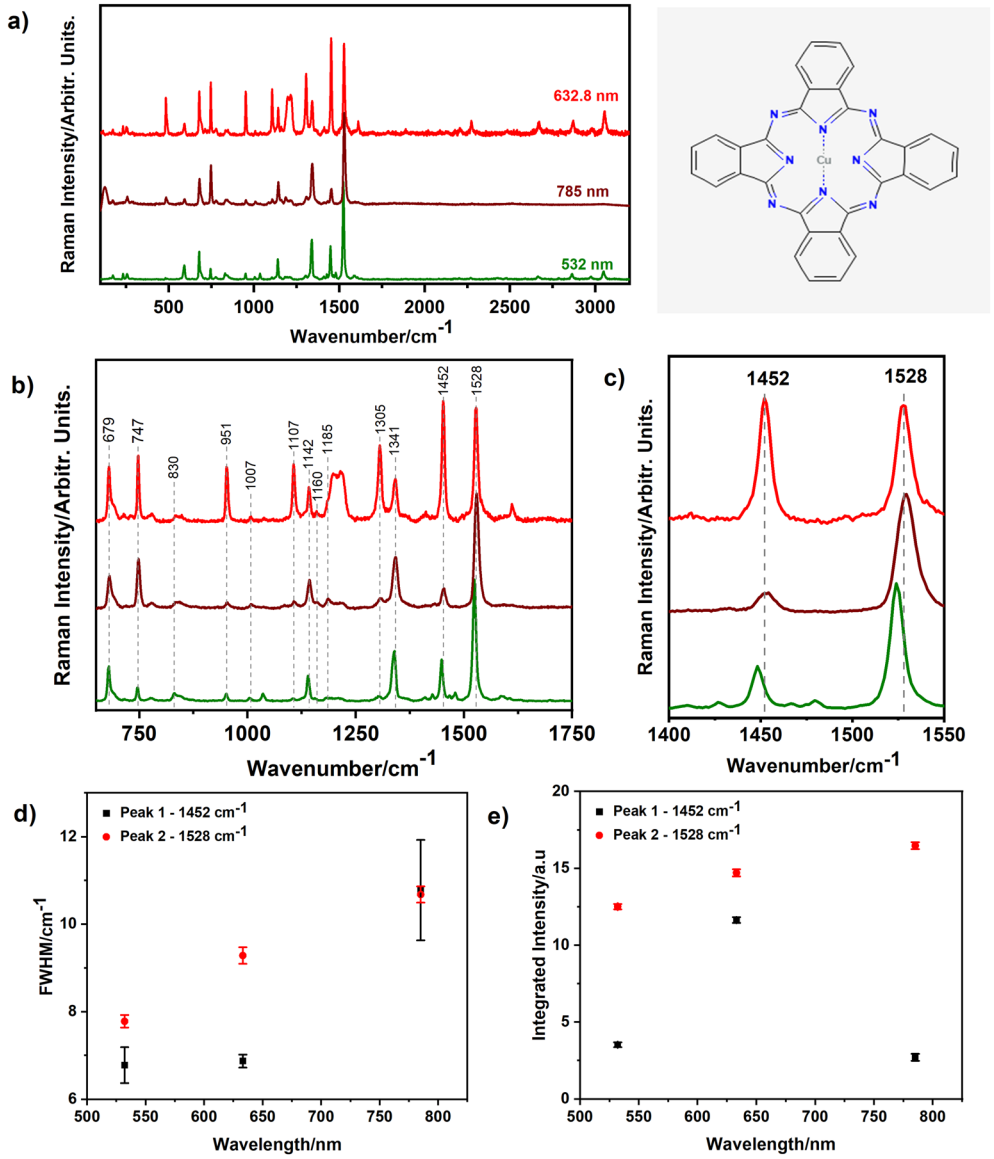

Fig. 2 Raman spectra of the CuPc pigment (the molecular structure is shown in the inset) at three excitation wavelengths, 632.8 nm, 785 nm and 532 nm, in the range of a) 100–3200 cm^{-1}, b) 600–1750 cm^{-1} and c) 1400–1550 cm^{-1}; and the variation of d) FWHM and e) integrated area values for the two highest intensity bands of CuPc, 1452 cm^{-1} and 1528 cm^{-1}, as a function of excitation wavelength; the error bars indicate standard deviation.

1750 cm^{-1}, respectively. The interval represented in Fig. 2b corresponds to the fingerprint region of PB15, which overlaps with the fingerprint region of polymers. Based on the excitation wavelength, there are differences in the PB15 signal, mostly in terms of the relative intensities of the bands. When using 532 nm and 785 nm excitation, Raman bands with rather similar relative intensity are obtained; however, as expected, when excited by a red laser at 632.8 nm (Fig. 2b), certain bands at 951 cm^{-1}, 1107 cm^{-1}, 1305 cm^{-1} and 1452 cm^{-1}, assigned[37,68] to pyrrole C=C, aza C–C stretches and isoindole deformation, are highly enhanced, as resonance conditions lead to increased Raman intensities for specific vibrational modes related to the chromophore of the pigment molecule. There are bands that are hardly noticeable under 532 nm and 785 nm excitation that when excited at 632.8 nm exhibit higher intensities and become distinctly visible. The corresponding bands are located at 951 cm^{-1}, 1107 cm^{-1}, and 1305 cm^{-1}. Apart from those, the most intense band at all wavelengths is at 1528 cm^{-1}, which is assigned to C–N–C stretches.[37]

The assignment of all the other copper phthalocyanine bands highlighted in Fig. 2b is discussed in detail by Harbeck and Mack.[70]

Further, we determined the variation of the FWHM (full width at half maximum) and integrated intensity dependence on the excitation wavelength for the two most intense bands of the PB15 pigment, 1452 cm^{-1} and 1528 cm^{-1}. The corresponding results are illustrated

in Fig. 2d and e. A slight shift of 1–2 cm^{-1} in band positions to higher wavenumbers and an increase in the FWHM with wavelength for both bands was noted, as expected, but the trend of increase is not similar. A significant increase in band intensity was observed upon excitation at 632.8 nm due to the resonance effect. It is observed that the integrated intensity of the band at 1452 cm^{-1} is noticeably higher upon 632.8 nm excitation and its intensity drops upon 785 nm excitation. The band at 1528 cm^{-1} showed a slightly increased integrated intensity with increasing excitation wavelength, due to its slight broadening.

Further, we were particularly interested in analyzing how the specific Raman signal of PB15 actually varies when it is combined with a polymer. Therefore, we measured blue macroplastics at three excitation wavelengths: 532 nm, 632.8 nm and 785 nm. The results obtained were grouped in three cases, as illustrated in Fig. 3.

The first case, exemplified by the sample HDPE-BL-001 in Fig. 3a, is characterized by high levels of difference in the Raman signals upon excitation. At 785 nm specific polymer bands are dominant, and the only bands specific to the PB15 pigment are the ones at 776 cm^{-1}, 1340 cm^{-1} and 1528 cm^{-1}. Conversely, with 632.8 nm excitation, both the pigment and polymer bands are clearly distinguishable. However, the bands specific to the pigment seem to dominate, with the strongest bands being at 776 cm^{-1} and 1528 cm^{-1}. Upon 532 nm excitation we could not record any signal, as the fluorescence was too intense. Moreover, we had also samples in the described collection that could not be analysed due to the fluorescence, even at 632.8 nm, as exemplified in Fig. S1.† for the sample PS-BL-001.

In the second case, as illustrated by the sample PP-BL-006 in Fig. 3b, specific signals from both the plastic and pigment are present and distinguishable when the excitation wavelength was 532 nm and 785 nm. In both spectra, the most intense band is at 1528 cm^{-1}, which corresponds to the PB15 pigment. When it comes to excitation at 632.8 nm, the pigment bands dominate while the plastic ones are barely visible.

In case three, as represented by the sample PP-BL-000 in Fig. 3c, the plastic bands are scarcely visible, particularly upon 532 nm and 632.8 nm excitation. Similar signals were collected upon 785 nm excitation, except that, in this case, two bands specific to the polymer (PP), at 809 cm^{-1} and 841 cm^{-1}, were visible. An interesting observation was that we got different signals from different measuring spots when using 632.8 nm excitation. As an example, Fig. 3c shows two Raman signals collected upon 632.8 nm excitation, and the results are very different. In one case the Raman signal is specific to the polymer and in the other case to the pigment. This finding suggests that the coloring of plastic items is not homogeneous over the entire polymer matrix, implying an inhomogeneous mixture of polymer and pigment. Therefore, as a result of fragmentation through environmental processes, the resulting particles could comprise either plastic, pigment, or both.

In conclusion, a consistent observation across all samples was that specific pigment bands were always visible when measurements were performed using the red laser at 632.8 nm for excitation. However, we observed that even if the pigment bands are clearly visible, the polymer bands are not always detectable; thus, the identification of the plastic species could be difficult. One alternative is to use the 785 nm laser, but this is to the detriment of spatial resolution, as detection is limited at sub-micrometer size. In addition, green laser excitation at 532 nm usually showed a higher fluorescence background, hampering accurate detection. Thus, when using the red laser at 632.8 nm for excitation, the detection of plastic particles was always possible due to the strong pigment signal, confirming the presence of blue plastics in the respective environmental matrix. Therefore, due to the resonance enhancement of the PB15 Raman signal, the detection of weakly scattering materials could be facilitated.

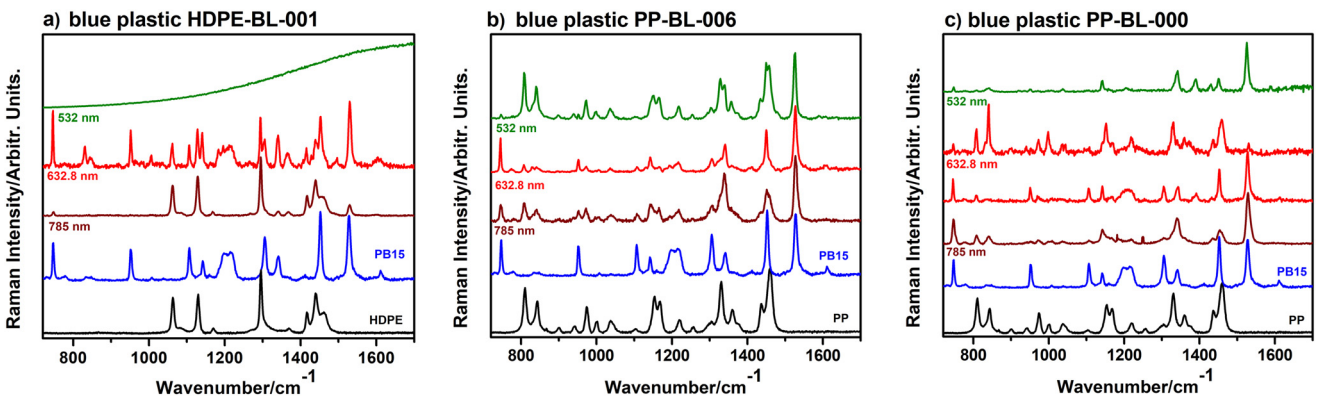

Fig. 3 Normalized Raman spectra of the blue plastics a) HDPE-BL-001, b) PP-BL-006 and c) PP-BL-000 at three excitation wavelengths: 532 nm (green line), 632.8 nm (red line), and 785 nm (dark red line); for the PP-BL-000 sample, two spectra are presented at 632.8 nm excitation, each corresponding to a different spot on the sample; the Raman spectrum of PB15 pigment (excitation: 632.8 nm) is given as a blue line for guidance, and the respective polymer spectrum is shown at the bottom as a black line for reference (excitation: 785 nm).

The abundance of the PB15 pigment in blue, naturally weathered macroplastics and microplastics

To assess the abundance of the PB15 pigment in blue and green plastics, we analyzed a collection of 107 blue plastic waste samples, including 26 blue and green macroplastics (20 blue, 5 green, and 1 turquoise) samples, covering five types of plastics – LDPE, HDPE, PS, PET and PP-and 81 blue microplastics (MPs) (Fig. 1). The macroplastics were naturally weathered samples and were gathered from different environmental matrices/compartments, where they were exposed to various degradation processes over a span of years. We additionally analyzed blue microplastics retained on several filters from stocks used for water filtration, as described above. The analysis was performed by means of micro-Raman spectroscopy using an excitation wavelength of 785 nm. We chose this wavelength for two reasons. First, when using this excitation wavelength, Raman signals are visible from both the pigment and polymer; secondly, we want to avoid fluorescence, as weathered/environmental plastics often exhibit fluorescence due to contaminant accumulation or the deposition of other biofilms. Given that Raman spectroscopy is a recognized method for detecting plastics, our investigation focused not only on the occurrence of PB15 in blue plastics but also on how the PB15 signal interferes with the identification process of macro- and microplastics.

We determined that, out of the 26 macroplastics, 21 presented the characteristic/distinctive Raman signal of PB15, in addition to the specific signal of the polymer, indicating a physical mixture of plastic and pigment. Hence, 81% of the samples (Fig. 4a) showed the addition of the PB15 pigment in the polymer matrix to give a blue or green color. The remaining 19% of the macroplastics only exhibited the specific polymer signal, without any trace of the PB15 pigment or any other pigment, despite their blue shade. This 19% of samples is exclusively blue, given that all the green and turquoise plastic samples exhibited the PB15 signal along with the specific Raman signal of the polymer (Fig. S2 in ESI†). Additionally, our analysis also revealed that out of the 21 blue and green macroplastics samples containing the PB15 pigment, 15 were identified as the PP plastic type.

However, upon further examination of the Raman signals from the 26 macroplastics, we determined that the specific signal of PB15 varies from one plastic type to another without a specific pattern, and we noticed variations even within the same type of polymer.

Fig. 5 illustrates the most representative spectra for each blue polymer type along with the Raman spectrum of the PB15 pigment for reference. The specific PB15 Raman signal is in the short-range spectra of the plastics (720 cm^{-1}–1800 cm^{-1}), with specific bands at 748 cm^{-1}, 953 cm^{-1}, 1142 cm^{-1}, 1340 cm^{-1}, 1452 cm^{-1} and 1528 cm^{-1}, the latter being the most intense one.

In the case of HDPE, not all the analyzed samples showed the PB15 signal. However, the ones that did show it, as exemplified by the sample HDPE-BL-001 in Fig. 5, presented the same three bands characteristic to PB15, at 748 cm^{-1}, 1340 cm^{-1} and 1528 cm^{-1}. The band at 1452 cm^{-1} overlaps with the PE band at 1460 cm^{-1}.

All blue PS macro-samples analyzed presented the PB15 signal, and it was similar for all the samples, as can be seen in Fig. 5 for PS-BL-001. Four bands characteristic to PB15 are visible, at 748 cm^{-1}, 953 cm^{-1}, 1340 cm^{-1} and 1528 cm^{-1}, and two bands, 1142 cm^{-1} and 1452 cm^{-1}, overlap with PS bands. However, even if we have these overlapping bands for PS and HDPE, the polymer identification process is not interfered with, as the main intense bands of the polymers are clearly seen for identification. To sum up, for both HDPE and PS, the most intense bands characteristic to PB15 were the ones at 748 cm^{-1} and 1528 cm^{-1}. However, their relative

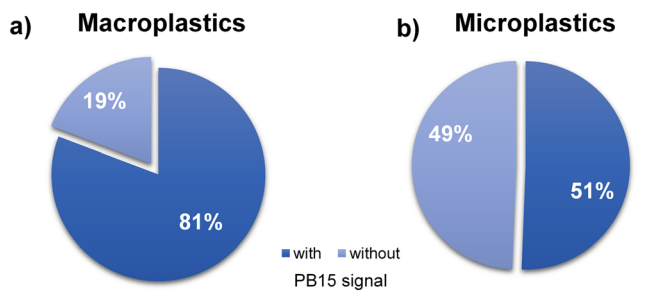

Fig. 4 The percentages of blue samples with and without the Raman signal specific to the PB15 pigment in the case of the a) macroplastics and b) microplastics analyzed.

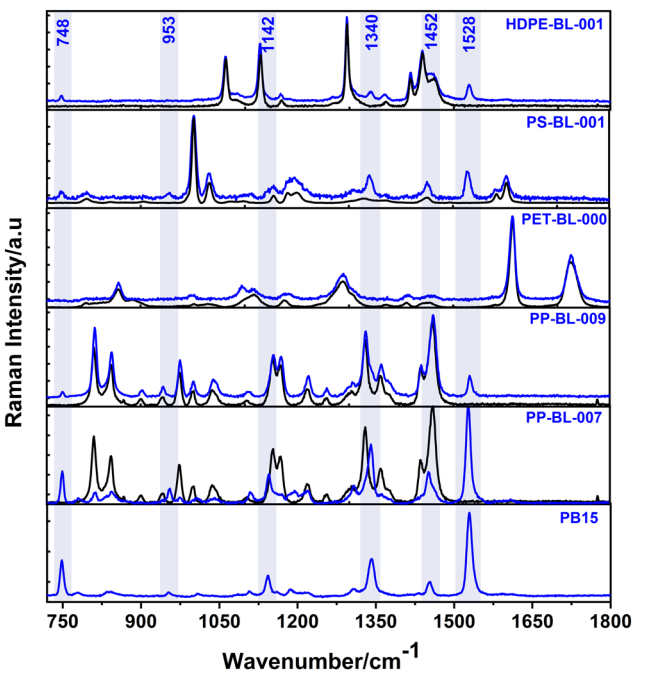

Fig. 5 Five of the most representative Raman spectra of blue macroplastics, along with corresponding reference spectrum, encompassing four types of plastics: HDPE, PS, PET and PP; except for the PET sample, all the other plastics revealed fingerprint bands from the PB15 signal; the bottom spectrum in blue corresponds to the PB15 pigment; excitation: 785 nm.

intensities are always weaker than those of the polymer bands, meaning the signal is still predominantly dominated by the polymer bands.

The blue PET macroplastics were an exception here, as they didn't exhibit the PB15 signal in their Raman signals. Therefore, the blue PET samples analyzed here were possibly colored with other inorganic pigments, possibly cobalt blue, which has known Raman bands at 514 cm^{-1} and 202 cm^{-1}. In the presented plastic samples, such bands were not detectable (the low spectral range is not shown here).

The Raman signal of the PB15 pigment was observed in all blue and green PP macro-samples analyzed, and nearly all the PB15 bands were present among the polymer ones. However, the PB15 signal varied significantly from one sample to another.

In Fig. 5, we illustrate the Raman signals of two PP samples, showing two distinct cases identified for PP. In the first case (exemplified by a blue polypropylene sample with the code PP-BL-007), the relative intensities of the PB15 bands were higher compared to the polymer bands. In the case of PP, two of the PB15 bands, 1340 cm^{-1} and 1528 cm^{-1}, overlap with the polymer bands. Moreover, specific bands of PP, notably at 908 cm^{-1} and 940 cm^{-1}, were clearly visible in the region between 900 and 1000 cm^{-1}, where the PB15 signal did not interfere.

In contrast, the second case (exemplified by a blue polypropylene sample with the code PP-BL-009) exhibited the opposite behavior, with the relative intensities of the PB15 bands being much lower than the polymer ones. Consequently, not all PB15 bands were as visible as in the first case. The most prominent PB15 bands in this case were at 748 cm^{-1} and 1528 cm^{-1}.

To sum up, our findings show that the PB15 signal was most frequently detected and varied the most in PP samples. We also noted that two specific bands of PB15, at 748 cm^{-1} and 1528 cm^{-1}, were consistently visible and distinguishable in samples that exhibited the PB15 signal. On the other hand, for samples that did not show the PB15 signal, we can infer that they were not colored with the PB15 pigment.

Regarding the blue weathered microplastics (Fig. 1b), their Raman signals exhibited distinct behavior compared to macroplastics. Among the 81 blue-color MPs analyzed, 41 (51%) presented the PB15 signal (Fig. 4b). The variability in the PB15 Raman signal of the 41 samples was further studied among the three microplastics batches. Starting with the microplastics originating from the spring water, the Raman signal specific to the polymer was barely visible. However, the few samples that presented the polymer signal were identified as PET due to the appearance of two characteristic PET bands, at 1614 cm^{-1} and 1725 cm^{-1} (exemplified by MP1 in Fig. 6a). Interestingly, even though only a few MPs showed specific polymer bands, the Raman spectra of the MPs were dominated by the PB15 signal, with 8 corresponding strong bands (748 cm^{-1}, 953 cm^{-1}, 1107 cm^{-1}, 1142 cm^{-1}, 1305 cm^{-1}, 1340 cm^{-1}, 1452 cm^{-1} and 1528 cm^{-1}), as can be observed for MP2 in Fig. 6a.

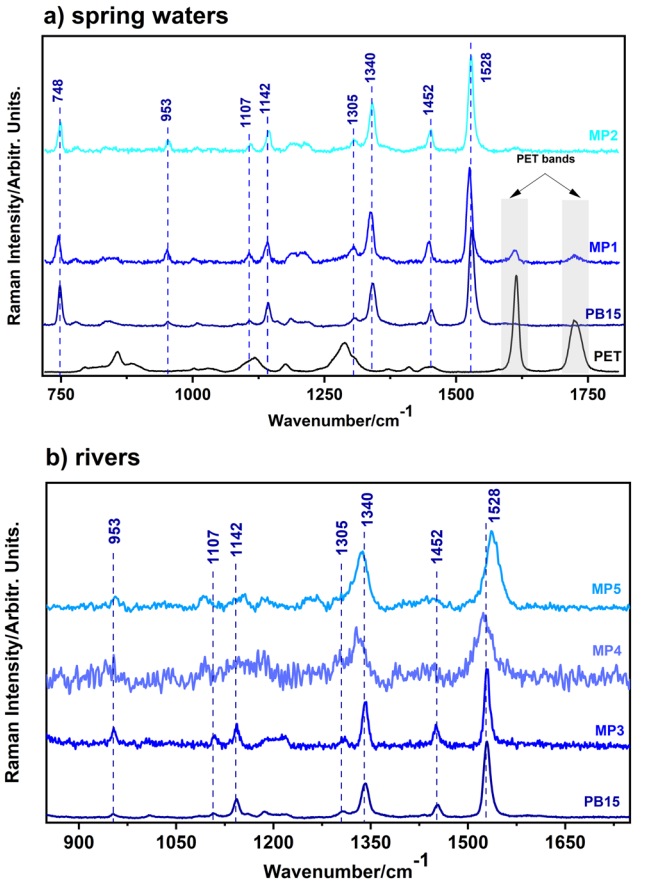

Fig. 6 Typical Raman spectra collected from abundantly observed blue fibers from two spring water sources (a) (Josani and Albioara, Romania) and two rivers (b) (Homorod and Somes, Romania); the spectra of PB15 and PET are given for reference; characteristic bands representing the highest intensity, although broadened, bands of Cu-phthalocyanine are observed (785 nm excitation).

In the case of MPs from rivers (Fig. 6b), no blue microplastics sample presented the polymer bands, thus, the plastic type was not detectable. All the blue MPs from the Somes river were characterized by a Raman signal specific only to the PB15 pigment (exemplified by MP3 in Fig. 6b). The Homorod river samples showed a similar picture – the only signal visible was characteristic to the PB15 pigment. Here, we identified two types of signals. The first one is exemplified by MP4, as shown in Fig. 6b, where only two bands specific to PB15 are clearly visible (1340 cm^{-1} and 1528 cm^{-1}). The second one (MP5 in Fig. 6b) is where more bands specific to PB15 appear, but there is a shift, especially for the band at 1528 cm^{-1}, indicating a change in the vibrational modes, and thus a possible slight chemical change in the pigment structure.

It is worth mentioning that interference in the Raman signal could arise from the carotenoids of aquatic microorganism biofilm attached to the plastic.[71] To check this, we analyzed a PET water bottle which was refilled with tap water and preserved for one year under lab conditions, resulting in the creation of a biofilm on the

bottle's inner surface. Analysis (Fig. S3†) revealed the formation of a biofilm from photosynthetic organisms on the interior surface of the bottle, whose Raman spectrum is characterized by a strong band at 1522 cm^{-1}, which is assigned to the –C═C– bonds of carotenoids, a band visible due to pre-resonance enhancement at 532 nm. Therefore, the photosynthetic organisms could interfere with the PB15 signal, which has the strongest band at 1528 cm^{-1}, particularly when diatom colonies are established. It is well-known[72] that diatoms exhibit a RR signal from their dominant fucoxanthin carotenoid, featuring a main C═C band at 1528 cm^{-1}, when 532 nm laser excitation is used. However, in this case, the profile of carotenoids and PB15 bands is different; therefore, they could be clearly differentiated.

In conclusion, the identification of MPs using Raman could indeed impose a great challenge for non-spectroscopists, as the characteristic plastic bands are barely seen compared to the pigment bands. However, as the PB15 signal is visible and strong, microparticles that show the PB15 signal can be identified as microplastics even if only the pigment bands are present. Therefore, the presence of PB15 in microplastics could be explored as an attractive analytical approach for tracing and monitoring the impact of micro-/nanoplastics on the environment using multiple excitations and combined Raman spectroscopy techniques.

PB15 screening in microplastics and nanoplastics at the single-particle level

To further demonstrate the possibility of PB15 screening, even in nanoplastics, *via* the pigment signature, we investigated one of our blue samples from our database, named PP-BL-003 (Fig. 1c). 15 years of degradation under aquatic conditions and 5 years of storage of this blue sample have resulted in a high susceptibility to fragmentation into smaller pieces of micrometer and nanometer sizes (Fig. 1d). Therefore, the micro- and nanoparticles analyzed further are environmentally relevant samples, as they are the result of natural degradation processes, such as photodegradation and thermo-oxidative degradation.[62] First, SEM–EDX measurements were conducted and the results are shown in Fig. 7 for two representative nanoparticles. Indeed, the presence of blue nanoparticles was confirmed, first based on size and then based on composition, where carbon and copper are dominant (the nickel signal is from the support used for SEM measurements). A few additional SEM/TEM images of blue nanoparticles are presented in Fig. 8a. We see that they have irregular shapes and they are attracted to each other, forming agglomerates. Further, for Raman analyses, a very small quantity of blue plastic powder was spread on a microscope slide (Fig. 8b). The particles dispersed on the slide, as seen in the microscope image in Fig. 8c, were

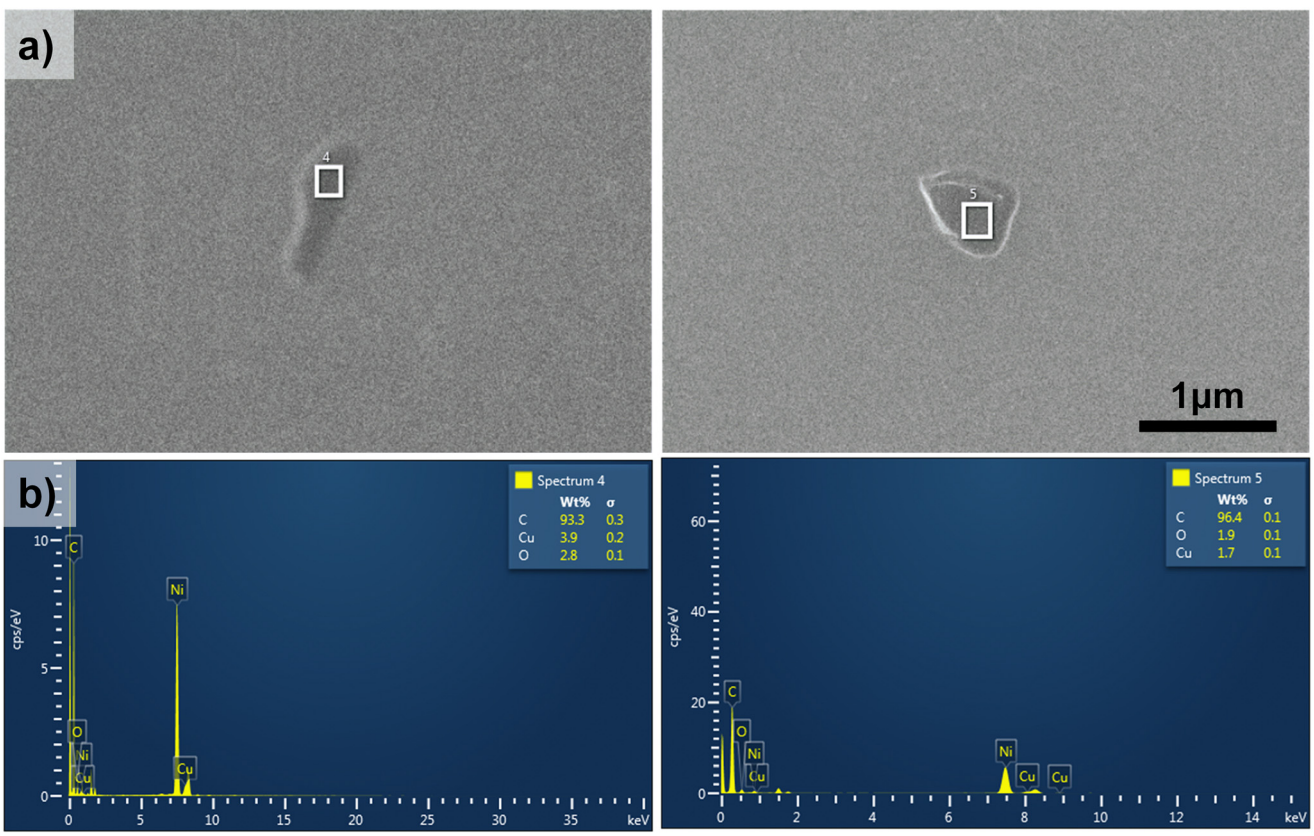

Fig. 7 SEM images (a) and the corresponding EDX measurements (b) for two representative blue nanoplastics.

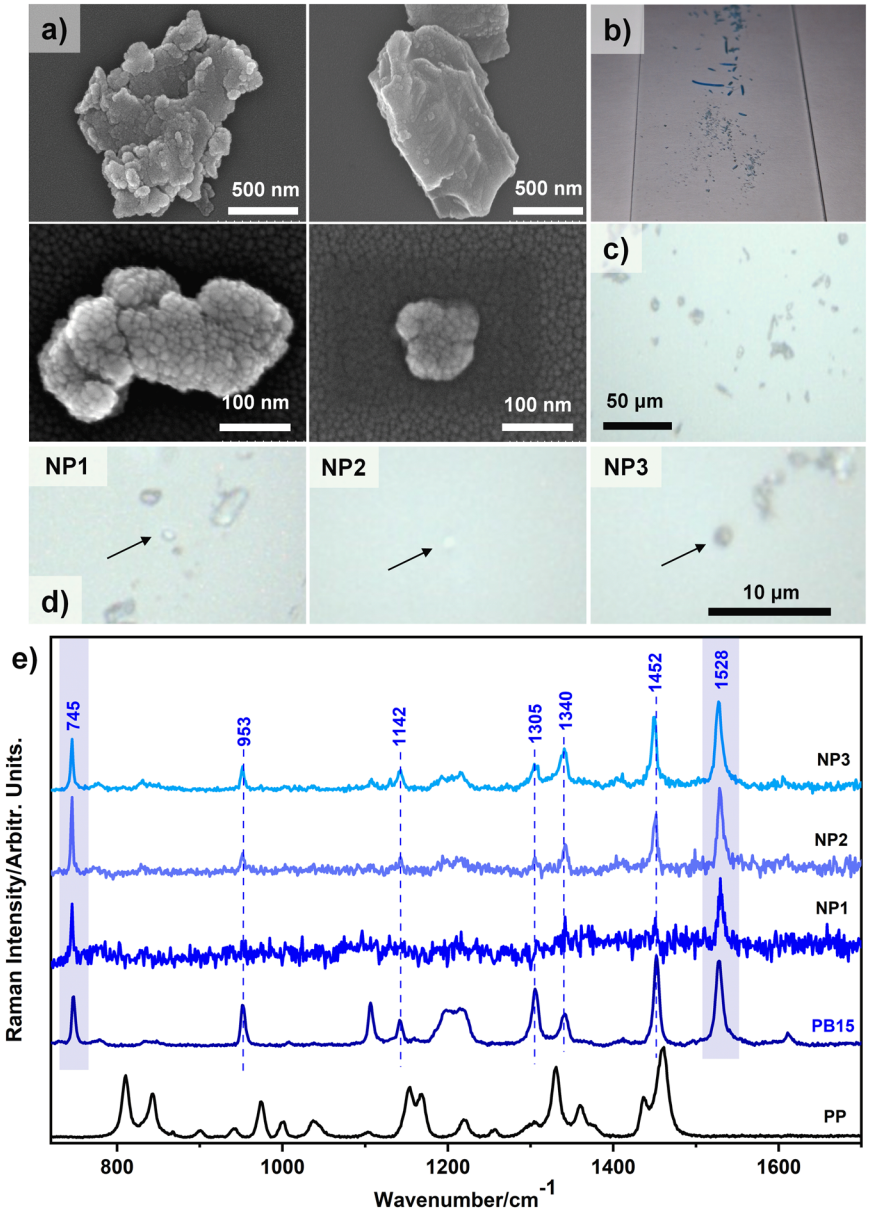

Fig. 8 a) SEM/TEM images of blue nanoplastics resulting from the fragmentation of the PP-BL-003 sample; b) macroscopic and c) optical microscopy images of the blue micro- and nanoplastic particles spread on a microscope slide; d) optical microscopy images of three blue nanoplastics (NP1, NP2 and NP3) and e) their corresponding Raman spectra (excitation: 632.8 nm) together with the spectra of PB15 pigment (excitation: 632.8 nm) and PP (excitation: 785 nm) for reference.

investigated *via* micro-Raman spectroscopy using a 100x magnification objective. Given the irregular shapes of these particles, we defined the dimensions of the particles considering the minimum Feret diameter. However, due to the sub-micrometer-size particles being barely visible under the microscope, it was challenging to determine their dimensions; thus, we made an estimation using *ImageJ* software. Using nanospheres with a known diameter as a reference, we observed that the particles seem larger than they are, due to the diffraction limit,[73] but here we reported correctly estimated values.

Before any other analyses, a macroplastic filament of this sample was investigated using three excitation wavelengths, and the results can be seen in Fig. S4 in the ESI.† With green and near-IR excitation, we can clearly see both signals, from the pigment and plastic, with the most intense band at 1528 cm^{-1}. However, when 632.8 nm excitation is used, the spectrum is predominantly characterized by the pigment bands.

After the analysis of the smallest particles visible under the microscope, we succeeded based on RR spectroscopy to detect sub-micrometer-size particles of blue plastic, *i.e.* nanoplastics. Fig. 8d shows images of three analyzed blue particles (NP1, NP2 and NP3) and Fig. 8e shows the corresponding resonance Raman signals collected with 632.8 nm excitation. NP1 and NP2 have an average Feret

diameter of 500 nm and that of NP3 is 800 nm. The Raman spectra of all three particles correspond to the specific signal of PB15, and there are no signs of any bands characteristic of the polymer (PP). Therefore, due to the enhanced resonance Raman signals, irrespective of the plastic, blue nanoplastic particles can be tracked in the environment *via* their pigment signature rather than their polymer signal.

Moreover, among all the particles analyzed, we also had samples that gave only the specific Raman signal of the plastic, in our case PP. The Raman spectra of three particles are given in Fig. S5 in the ESI.† The average Feret diameters of MP1, MP2 and MP3 are 1.2 μm, 900 nm, and 650 nm, respectively. This again indicates, as we saw for macro- and microplastics above, that the plastics are not uniformly colored, suggesting that the pigment is not distributed uniformly within the polymer volume. Thus, in the results from naturally fragmented PP-BL-003 filaments, there could be a variation in the CuPc pigment content in the resulting nanoplastics. This behavior was also confirmed *via* SEM–EDX measurements, where the ratio of carbon to copper varied from particle to particle (Fig. S6†), where copper detection indicated that the respective nanoplastic is blue. However, the release of additives, including pigments, is expected to happen for nanoplastics due to their increased specific surface area.[73,74]

Furthermore, we analyzed blue particles at all three excitation wavelengths, and Fig. S7† shows the representative spectral results obtained for a particle with the average Feret diameter of 1 μm. Excitation at 785 nm was not effective for recording any Raman signal, as expected. In this regard, we tested additional larger particles of a few micrometers in size, which promptly provided the specific Raman signals of both the pigment and plastic. With 632.8 nm excitation, the specific Raman signal of PB15 was dominant. Conversely, at 532 nm we obtained nice signals from both the pigment and plastics. In this regard, a green laser seems to be a better alternative than excitation at 632.8 nm when the identification of the particle is needed, as we also obtained the polymer signal. However, we should take into consideration that most plastic samples, especially environmental ones, are prone to fluorescence. Therefore, the best choice bearing in mind any necessary compromise is to use 632.8 nm excitation, as it falls within the resonance spectral region.[73]

Notably, any blue fragments or fibers within the sub-micrometer range could potentially derive from objects other than plastics, such as vegetal or animal-based blue-dyed fibers, or flakes from degraded paint, textiles, coatings, or inks. It must be pointed out that wool, cashmere, silk, linen and other fibers of animal or vegetal origin are well-known protein-based or cellulose-based, respectively, structures with typical Raman signatures.[75] Supposing they occur in the same nanosized debris as suspected blue plastic particles, their blue coloration is quite different, based on protein-reactive dyes, such as the water-soluble and anionic acid blue 25, with an anthraquinone skeletal structure or widely used indigo, as we earlier showed in our investigation of an Italian cultural heritage canvas dyed with a limited palette of white, green and blue.[76]

When micro-/nanoplastics are taken up by living organisms, the plastic effects are generally investigated, but chemical toxicity from leachates in the presence of the plastic is hidden, thus, they can be the subject of further studies. The blue plastic intake is metaphorized in the title of the present paper as a "strategy to infiltrate" (or Trojan horse). In a broader sense, the term "Trojan horse" can be used metaphorically to describe any strategy that hides its true intent. A "Trojan horse" can thus refer to an action or object that appears harmless or beneficial but has a hidden action or a subsequent, additional effect. This study provides comprehensive data to further use such a Trojan horse based on blue micro-/nanoplastics to use RR tools to track plastic intake and its fate in living (micro)organisms.

In conclusion, abundantly found blue nanoplastics comprising the widely used PB15 industrial pigment offer a great analytical alternative for monitoring blue micro- and nanoplastics in various environmental matrices based on the pigment's specific and intense resonance Raman signal in respective plastic samples.

Conclusions

Despite the growing interest in nanoplastics, the detection of environmentally aged nanoplastics has barely been addressed in the literature, as there is no reliable analytical technique to detect and track nanoplastics in environmental matrices.

The present work showed for the first time that micro-Raman spectroscopy combined with resonance Raman analysis of blue-pigmented plastics aged in natural aquatic environments provides a robust analytical alternative for the detection of highly abundant blue nanoplastics at the single-particle level.

In this study we made use of naturally aged blue polypropylene (PP), the second-most abundant plastic pollutant worldwide, coloured blue with the copper phthalocyanine (CuPc) pigment, which exhibits a particular resonance Raman (RR) signal under appropriate laser excitation. Thus, by leveraging the newly discovered resonance Raman (RR) signal of the CuPc blue pigment, we successfully detected and tracked fibrous and fragmentary blue nanoplastics down to a size of 500 nm. By lowering the minimal size (previously known to be 1 μm) of nanoplastics detectable using Raman spectroscopy, the performance of the Raman technique was improved, contributing to its validation as a standard technique for nano- and microplastics detection.

The analytical approach presented here could be exploited further for tracing and monitoring blue nanoplastics accumulation and transmission in the food web or trophic chains, with an impact on currently proposed regulations still to be implemented.

Data availability

The data supporting this article have been included as part of the ESI.†

Author contributions

Ioana Cârdan: conceptualization, data curation, formal analysis, investigation, methodology, visualization, writing – original draft, writing – review & editing. Ion Nesterovschi: data curation, investigation, formal analysis. Lucian Barbu-Tudoran: investigation, data curation, formal analysis Simona Cîntă Pînzaru: conceptualization, methodology, data curation, supervision, writing – review & editing.

Conflicts of interest

There are no conflicts of interest to declare.

Acknowledgements

I. C. acknowledges the fellowship granted by Babeş-Bolyai University through the project STAR-UBB-N, ID: PFE-550-UBB, contract no. 21PFE/30.12.2021. The authors deeply acknowledge Dr. Luiza Gaina from the Department of Chemistry, Faculty of Chemistry and Chemical Engineering, Babes-Bolyai University, Cluj-Napoca, Romania for providing the solid copper phthalocyanine pigment for this study.

References

1 *ISO/TR 21960:2020 - Plastics — Environmental aspects — State of knowledge and methodologies*, **https://www.iso.org/standard/72300.html** (accessed 16 May2024).
2 S. Sangkham, O. Faikhaw, N. Munkong, P. Sakunkoo, C. Arunlertaree and M. Chavali, *et al.*, A review on microplastics and nanoplastics in the environment: Their occurrence, exposure routes, toxic studies, and potential effects on human health, *Mar. Pollut. Bull.*, 2022, **181**, 113832.
3 H. A. Leslie, M. J. M. van Velzen, S. H. Brandsma, A. D. Vethaak, J. J. Garcia-Vallejo and M. H. Lamoree, Discovery and quantification of plastic particle pollution in human blood, *Environ. Int.*, 2022, **163**, 107199.
4 A. Ragusa, A. Svelato, C. Santacroce, P. Catalano, V. Notarstefano and O. Carnevali, *et al.*, Plasticenta: First evidence of microplastics in human placenta, *Environ. Int.*, 2021, **146**, 106274.
5 M. Cole, P. Lindeque, E. Fileman, C. Halsband, R. Goodhead and J. Moger, Microplastic ingestion by zooplankton, *Environ. Sci. Technol.*, 2013, **47**, 6646–6655.
6 C. J. Thiele, M. D. Hudson, A. E. Russell, M. Saluveer and G. Sidaoui-Haddad, Microplastics in fish and fishmeal: an emerging environmental challenge?, *Sci. Rep.*, 2021, **11**(1), 1–12.
7 J. Wu, M. Lai, Y. Zhang, J. Li, H. Zhou and R. Jiang, Microplastics in the digestive tracts of commercial fish from the marine ranching in east China sea, China, *Case Stud. Chem. Environ. Eng.*, 2020, **2**, 100066.
8 R. C. Moore, M. Noel, A. Etemadifar, L. Loseto, A. M. Posacka and L. Bendell, Microplastics in beluga whale (Delphinapterus leucas) prey: An exploratory assessment of trophic transfer in the Beaufort Sea, *Sci. Total Environ.*, 2022, **806**, 150201.
9 I. Goßmann, D. Herzke, A. Held, J. Schulz, V. Nikiforov and C. Georgi, *et al.*, Occurrence and backtracking of microplastic mass loads including tire wear particles in northern Atlantic air, *Nat. Commun.*, 2023, **14**, 1–9.
10 C. Campanale, S. Galafassi, I. Savino, C. Massarelli, V. Ancona and P. Volta, *et al.*, Microplastics pollution in the terrestrial environments: Poorly known diffuse sources and implications for plants, *Sci. Total Environ.*, 2022, **805**, 150431.
11 I. Nesterovschi, I. Marica, E. Andrea Levei, S. Bogdan Angyus, M. Kenesz and O. Teodora Moldovan, *et al.*, Subterranean transport of microplastics as evidenced in karst springs and their characterization using Raman spectroscopy, *Spectrochim. Acta, Part A*, 2023, **298**, 122811.
12 D. K. Gupta, D. Choudhary, A. Vishwakarma, M. Mudgal, A. K. Srivastava and A. Singh, Microplastics in freshwater environment: occurrence, analysis, impact, control measures and challenges, *Int. J. Environ. Sci. Technol.*, 2022, **20**, 6865–6896.
13 J. Stanković, D. Milošević, M. Paunović, B. Jovanović, N. Popović and J. Tomović, Microplastics in the Danube River and Its Main Tributaries—Ingestion by Freshwater Macroinvertebrates, *Water*, 2024, **16**, 962.
14 I. V. Kirstein, A. Gomiero and J. Vollertsen, Microplastic pollution in drinking water, *Curr. Opin. Toxicol.*, 2021, **28**, 70–75.
15 J. Zhang, M. Peng, E. Lian, L. Xia, A. G. Asimakopoulos and S. Luo, *et al.*, Identification of Poly(ethylene terephthalate) Nanoplastics in Commercially Bottled Drinking Water Using Surface-Enhanced Raman Spectroscopy, *Environ. Sci. Technol.*, 2023, **57**, 8365–8372.
16 N. Qian, X. Gao, X. Lang, H. Deng, T. M. Bratu, Q. Chen, B. Yan and W. Min, Rapid single-particle chemical imaging of nanoplastics by SRS microscopy, *Proc. Natl. Acad. Sci. U. S. A.*, 2024, **121**, e2300582121.
17 L. E. Medina Faull, T. Zaliznyak and G. T. Taylor, From the Caribbean to the Arctic, the most abundant microplastic particles in the ocean have escaped detection, *Mar. Pollut. Bull.*, 2024, **202**, 116338.
18 D. A. Utami, L. Reuning, L. Schwark, G. Friedrichs, L. Dittmer and A. U. Nurhidayati, *et al.*, Plastiglomerates from uncontrolled burning of plastic waste on Indonesian beaches contain high contents of organic pollutants, *Sci. Rep.*, 2023, **13**, 1–12.
19 M. Perraki, V. Skliros, P. Mecaj, E. Vasileiou, C. Salmas and I. Papanikolaou, *et al.*, Identification of Microplastics Using μ-Raman Spectroscopy in Surface and Groundwater Bodies of SE Attica, Greece, *Water*, 2024, **16**, 843.
20 T. Babos, C. Lazar, O. Dobre, C. Pop and I. Pojar, Microplastic characterization in Romanian coastal waters, Western Black Sea, *Geoecomarina*, 2023, **29**, 51–58.

21 I. Chakraborty, S. Banik, R. Biswas, T. Yamamoto, H. Noothalapati and N. Mazumder, Raman spectroscopy for microplastic detection in water sources: a systematic review, *Int. J. Environ. Sci. Technol.*, 2023, **20**, 10435–10448.
22 J. Wu, M. Lai, Y. Zhang, J. Li, H. Zhou and R. Jiang, *et al.*, Microplastics in the digestive tracts of commercial fish from the marine ranching in east China sea, China, *Case Stud. Chem. Environ. Eng.*, 2020, **2**, 100066.
23 J. Stanković, D. Milošević, M. Paunović, B. Jovanović, N. Popović and J. Tomović, *et al.*, Microplastics in the Danube River and Its Main Tributaries—Ingestion by Freshwater Macroinvertebrates, *Water*, 2024, **16**, 962.
24 E. Martí, C. Martin, M. Galli, F. Echevarría, C. M. Duarte and A. Cózar, The Colors of the Ocean Plastics, *Environ. Sci. Technol.*, 2020, **54**, 6594–6601.
25 S. Rytelewska and A. D. Abrowska, The Raman Spectroscopy Approach to Different Freshwater Microplastics and Quantitative Characterization of Polyethylene Aged in the Environment, *Microplastics*, 2022, **1**, 263–281.
26 R. Lenz, K. Enders, C. A. Stedmon, D. M. A. MacKenzie and T. G. Nielsen, A critical assessment of visual identification of marine microplastic using Raman spectroscopy for analysis improvement, *Mar. Pollut. Bull.*, 2015, **100**, 82–91.
27 G. Lamichhane, A. Acharya, R. Marahatha, B. Modi, R. Paudel and A. Adhikari, *et al.*, Microplastics in environment: global concern, challenges, and controlling measures, *Int. J. Environ. Sci. Technol.*, 2022, **20**, 4673–4694.
28 *ROMÂNIA, TE IUBESC! - ROMÂNIA LA PET*, PROTV documentary, 2022, **https://www.youtube.com/watch?v=DYb3MtMRwMk&t=423s&ab_channel=ROMANIA%2CTEIUBESC%21** (accessed 27 May2024).
29 J. M. Robertson, 136. An X-ray study of the structure of the phthalocyanines. Part I. The metal-free, nickel, copper, and platinum compounds, *J. Chem. Soc.*, 1935, 615–621.
30 R. Christie, *Colour Chemistry*, Royal Society of Chemistry, 2014.
31 P. Gregory, Industrial applications of phthalocyanines, *J. Porphyrins Phthalocyanines*, 2000, **4**, 432–437.
32 P. Erk and H. Hengelsberg, Phthalocyanine Dyes and Pigments, *The Porphyrin Handbook: Multporphyrins, Multiphthalocyanines and Arrays*, 2003, vol. 19, pp. 105–149.
33 D. Wöhrle, G. Schnurpfeil, S. G. Makarov, A. Kazarin and O. N. Suvorova, Practical Applications of Phthalocyanines – from Dyes and Pigments to Materials for Optical, Electronic and Photo-electronic Devices, *Macroheterocycles*, 2012, **5**, 191–202.
34 R. Christie and A. Abel, Phthalocyanine blue pigments, *Phys. Sci. Rev.*, 2021, **6**, 391–404.
35 P. Gregory, Metal Complexes as Speciality Dyes and Pigments, *Comprehensive Coordination Chemistry II*, 2003, vol. 9, pp. 549–579.
36 J. R. Fryer, R. B. McKay, R. R. Mather and K. S. W. Sing, The technological importance of the crystallographic and surface properties of copper phthalocyanine pigments, *J. Chem. Technol. Biotechnol.*, 1981, **31**, 371–387.
37 W. Fremout and S. Saverwyns, Identification of synthetic organic pigments: the role of a comprehensive digital Raman spectral library, *J. Raman Spectrosc.*, 2012, **43**, 1536–1544.
38 Z. Tianyong and Z. Chunlong, Properties of copper phthalocyanine blue (C.I. Pigment Blue 15:3) treated with poly(ethylene glycol)s, *Dyes Pigm.*, 1997, **35**, 123–130.
39 P. A. Lewis, Colored Organic Pigments, *Applied Polymer Science: 21st Century*, 2000, pp. 493–526.
40 G. Zeng, M. Dai, P. Liu, T. Chen, L. Hu and H. Luo, *et al.*, Phthalocyanine blue leaching and exposure effects on Microcystis aeruginosa (cyanobacteria) of photoaged microplastics, *J. Hazard. Mater.*, 2024, **469**, 133984.
41 E. Martí, C. Martin, M. Galli, F. Echevarría, C. M. Duarte and A. Cózar, The Colors of the Ocean Plastics, *Environ. Sci. Technol.*, 2020, **54**, 6594–6601.
42 D. G. Shaw and R. H. Day, Colour- and form-dependent loss of plastic micro-debris from the North Pacific Ocean, *Mar. Pollut. Bull.*, 1994, **28**, 39–43.
43 V. Allen, J. H. Kalivas and R. G. Rodriguez, Post-Consumer Plastic Identification Using Raman, *Spectroscopy*, 2016, **53**, 672–681, DOI: **10.1366/0003702991947324**.
44 A. Tsuchida, H. Kawazumi, A. Kazuyoshi and T. Yasuo, Identification of shredded plastics in milliseconds using raman spectroscopy for recycling, *Proc. IEEE Sens.*, 2009, 1473–1476.
45 I. Marica, M. Aluaș and P. S. Cîntă, Raman technology application for plastic waste management aligned with FAIR principle to support the forthcoming plastic and environment initiatives, *Waste Manage.*, 2022, **144**, 479–489.
46 A. I. Marica, M. Aluas and S. C. Pinzaru, The management and stewardship of medical plastic waste using raman spectroscopy to sustain circular economy, *2019 7th E-Health and Bioengineering Conference*, EHB 2019, 2019, DOI: **10.1109/EHB47216.2019.8970076**.
47 H. Kawazumi, A. Tsuchida, T. Yoshida and Y. Tsuchida, High-performance recycling system for waste plastics using raman identification, in: *Progress in Sustainable Energy Technologies Vol II: Creating Sustainable Development*, 2014, DOI: **10.1007/978-3-319-07977-6_34**.
48 C. F. Araujo, M. M. Nolasco, A. M. P. Ribeiro and P. J. A. Ribeiro-Claro, Identification of microplastics using Raman spectroscopy: Latest developments and future prospects, *Water Res.*, 2018, **142**, 426–440.
49 H. Cai, E. G. Xu, F. Du, R. Li, J. Liu and H. Shi, Analysis of environmental nanoplastics: Progress and challenges, *Chem. Eng. J.*, 2021, **410**, 128208.
50 A. Ciorîță, M. Suciu, A. M. Rostas, A. Tarța, G. Popovici and M. Bocăneală, *et al.*, Interaction of Low-Density Polyethylene Nanofragments with Autotrophic and Chemotrophic Bacteria, *ACS Sustainable Chem. Eng.*, 2024, **12**, 10831–10840.
51 L. D. B. Mandemaker and F. Meirer, Spectro-Microscopic Techniques for Studying Nanoplastics in the Environment and in Organisms, *Angew. Chem., Int. Ed.*, 2023, **62**, e202210494.
52 *Directive - 2020/2184 - EN - EUR-Lex*, **https://eur-lex.europa.eu/eli/dir/2020/2184/oj** (accessed 27 May2024).

53 A. Käppler, D. Fischer, S. Oberbeckmann, G. Schernewski, M. Labrenz and K. J. Eichhorn, *et al.*, Analysis of environmental microplastics by vibrational microspectroscopy: FTIR, Raman or both?, *Anal. Bioanal. Chem.*, 2016, **408**, 8377–8391.

54 J. Caldwell, L. Rodriguez-Lorenzo, B. Espiña, A. Beck, F. Stock and K. Voges, *et al.*, Detection of submicron- and nanoplastics spiked in environmental fresh- and saltwater with Raman spectroscopy, *Mar. Pollut. Bull.*, 2024, **203**, 116468.

55 R. S. Das and Y. K. Agrawal, Raman spectroscopy: Recent advancements, techniques and applications, *Vib. Spectrosc.*, 2011, **57**, 163–176.

56 R. R. Jones, D. C. Hooper, L. Zhang, D. Wolverson and V. K. Valev, Raman Techniques: Fundamentals and Frontiers, *Nanoscale Res. Lett.*, 2019, **14**, 1–34.

57 J. Caldwell, P. Taladriz-Blanco, L. Rodriguez-Lorenzo, B. Rothen-Rutishauser and A. Petri-Fink, Submicron- and nanoplastic detection at low micro- to nanogram concentrations using gold nanostar-based surface-enhanced Raman scattering (SERS) substrates, *Environ. Sci.:Nano*, 2024, **11**, 1000–1011.

58 L. Chang, S. Jiang, J. Luo, J. Zhang, X. Liu and C. Y. Lee, *et al.*, Nanowell-enhanced Raman spectroscopy enables the visualization and quantification of nanoplastics in the environment, *Environ. Sci.:Nano*, 2022, **9**, 542–553.

59 R. Borlan, D. Stoia, L. Gaina, A. Campu, G. Marc and M. Perde-Schrepler, *et al.*, Fluorescent Phthalocyanine-Encapsulated Bovine Serum Albumin Nanoparticles: Their Deployment as Therapeutic Agents in the NIR Region, *Molecules*, 2021, **26**, 4679.

60 I. Marica and S. C. Pînzaru, A Raman spectral database of naturally aged plastics: A proof-of-concept study for waste plastic sorting, *J. Raman Spectrosc.*, 2023, **54**, 305–313.

61 I. Marica and S. Pinzaru, *Plastic Raman Database – A Raman spectral database of aged plastics*, 2021, https://plasticramandatabase.phys.ubbcluj.ro/ (accessed 26 May2024).

62 A. L. Andrady, Microplastics in the marine environment, *Mar. Pollut. Bull.*, 2011, **62**, 1596–1605.

63 S. N. Dimassi, J. N. Hahladakis, M. N. D. Yahia, M. I. Ahmad, S. Sayadi and M. A. Al-Ghouti, Degradation-fragmentation of marine plastic waste and their environmental implications: A critical review, *Arabian J. Chem.*, 2022, **15**, 104262.

64 S. D. Velioglu, E. Ercioglu, H. T. Temiz, H. M. Velioglu, A. Topcu and I. H. Boyaci, Raman Spectroscopic Barcode Use for Differentiation of Vegetable Oils and Determination of Their Major Fatty Acid Composition, *J. Am. Oil Chem. Soc.*, 2016, **93**, 627–635.

65 B. W. Caplins, T. K. Mullenbach, R. J. Holmes and D. A. Blank, Femtosecond to nanosecond excited state dynamics of vapor deposited copper phthalocyanine thin films, *Phys. Chem. Chem. Phys.*, 2016, **18**, 11454–11459.

66 N. Touka, H. Benelmadjat, B. Boudine, O. Halimi and M. Sebais, Copper phthalocyanine nanocrystals embedded into polymer host: Preparation and structural characterization, *J. Assoc. Arab Univ. Basic Appl. Sci.*, 2013, **13**, 52–56.

67 M. Szybowicz, T. Runka, M. Drozdowski, W. Bała, A. Grodzicki and P. Piszczek, *et al.*, High temperature study of FT-IR and Raman scattering spectra of vacuum deposited CuPc thin films, *J. Mol. Struct.*, 2004, **704**, 107–113.

68 C. Li, L. Zhang, M. Yang, H. Wang and Y. Wang, Dynamic and steady-state behaviors of reverse saturable absorption in metallophthalocyanine, *Phys. Rev. A: At., Mol., Opt. Phys.*, 1994, **49**, 1149.

69 N. B. McKeown, *Phthalocyanine materials : synthesis, structure, and function*, 1998, p. 193.

70 S. Harbeck and H. Mack, *Experimental and Theoretical Investigations on the IR and Raman Spectra for CuPc and TiOPc*, University of Tubingen, 2013, pp. 1–19.

71 *Chemistry in Pictures: Please wash your water bottle*, **https://cen.acs.org/environment/water/Chemistry-Pictures-Please-wash-water/102/web/2024/06** (accessed 10 Jul2024).

72 F. Nekvapil, I. Brezestean, G. Lazar, C. Firta and S. C. Pinzaru, Resonance Raman and SERRS of fucoxanthin: Prospects for carotenoid quantification in live diatom cells, *J. Mol. Struct.*, 2022, **1250**, 131608.

73 C. Fang, Z. Sobhani, X. Zhang, C. T. Gibson, Y. Tang and R. Naidu, Identification and visualisation of microplastics/nanoplastics by Raman imaging (ii): Smaller than the diffraction limit of laser?, *Water Res.*, 2020, **183**, 116046.

74 S. L. Wright and F. J. Kelly, Plastic and Human Health: A Micro Issue?, *Environ. Sci. Technol.*, 2017, **51**, 6634–6647.

75 D. Puchowicz, M. Cieslak, D. Puchowicz and M. Cieslak, Raman Spectroscopy in the Analysis of Textile Structures, *Recent Developments in Atomic Force Microscopy and Raman Spectroscopy for Materials Characterization*, 2021, DOI: **10.5772/INTECHOPEN.99731**.

76 O. M. Gui, A. Fălămaş, L. Barbu-Tudoran, M. Aluaş, B. Giambra and P. S. Cîntă, Surface-enhanced Raman scattering (SERS) and complementary techniques applied for the investigation of an Italian cultural heritage canvas, *J. Raman Spectrosc.*, 2013, **44**, 277–282.

